Inorganica Chimica Acta 366 (2011) 191–197

Contents lists available at ScienceDirect

Inorganica Chimica Acta

journal homepage: www.elsevier.com/locate/ica

Mono- and dinuclear Fe(III) complexes with the N_2O_2 donor 5-chlorosalicylideneimine ligands; synthesis, X-ray structural characterization and magnetic properties

Yasemin Yahsi [a,*], Hulya Kara [a], Lorenzo Sorace [b], Orhan Buyukgungor [c]

[a] Balıkesir University, Faculty of Art and Science, Department of Physics, TR 10145 Balıkesir, Turkey
[b] Dipartimento di Chimica and UdR INSTM, Universita' di Firenze, Firenze, Italy
[c] Ondokuz Mayıs University, Faculty of Art and Science, Department of Physics, Samsun, Turkey

ARTICLE INFO

Article history:
Received 25 June 2010
Received in revised form 19 October 2010
Accepted 26 October 2010
Available online 11 November 2010

Keywords:
Schiff-base ligands
N_2O_2 donors
Iron(III) complexes
X-ray crystal structure analysis
Magnetic properties

ABSTRACT

Two novel monomeric $[C_{18}H_{17}Cl_3N_2O_2Fe]$ (**1**) and dimeric $[C_{38}H_{36}N_4O_4Cl_6Fe_2]$ (**2**) Fe(III) tetradentate Schiff base complexes have been synthesized and their crystal structures have been determined by single crystal X-ray diffraction analysis. In complex (**1**) the Schiff base ligand coordinates toward one iron atom in a tetradentate mode and each iron atom is five coordinated with the coordination geometry around iron atom which can be described as a distorted square pyramid. The presence of a short (2.89 Å) non-bonding interatomic Fe···O distances between adjacent monomeric Fe(III) complexes results in the formation of a dimer. Structural analysis of compound (**2**) shows that the structure is a centrosymmetric dimer in which the six coordinated Fe(III) atoms are linked by μ-phenoxo bridges from one of the phenolic oxygen atoms of each Schiff base ligand to the opposite metal center. The variable-temperature (2–300 K) magnetic susceptibility (χ) data of these two compounds have been investigated. The results show that for both complexes Fe(III) centers are in the high spin configuration ($S = 5/2$) and indicate antiferromagnetic spin-exchange interaction between Fe(III) ions. The obtained results are briefly discussed using magnetostructural correlations developed for other class of iron(III) complexes.

1. Introduction

Since several decades, structural, magnetic and spectroscopic properties of Schiff base complexes have been studied extensively [1–3]. The design, synthesis and characterization of iron complexes with salicylaldimine Schiff-base ligands (Scheme 1) play an important role in the fields of bioinorganic, organometallic, and catalytic chemistry due to their importance as synthetic models for the iron-containing enzymes [4,5], oxidation catalysts [6–9] and bistable molecular materials based on temperature-, pressure- or light-induced spin-crossover behavior [10–16]. Additionally, dinuclear complexes were treated as models for understanding the effect of structural parameters in determining the size and magnitude of exchange coupling interactions between the two iron centers [17].

However, while these studies clearly showed that hydroxo-, alkoxo- and phenoxo-bridges are accountable for weak antiferromagnetic coupling and oxo-bridged complexes are strongly coupled [18–21], the effect of each specific geometrical parameter (Fe–O bond distances, Fe–O–Fe bond angle and Fe···Fe distance) on the superexchange integral in Fe_2O_2 bridging systems, is not yet understood in detail due to absence of adequate crystal structure data.

Among dinuclear systems, we are currently interested in the synthesis and characterization of phenolate oxygen-bridged diiron Schiff-base complexes. It is indeed interesting to note that, up to date, only for a few complexes of this family have the X-ray structure been solved [20–29] and even less have been characterized by magnetic studies. The expansion of the number of the complexes characterized both structurally and magnetically is then a prerequisite to develop further magnetostructural correlation for iron(III) oxygen bridged dimers. Our aim is to understand the effect of geometric parameters, including the layout of the Fe(III) ions and bridging oxygen atoms on the super-exchange interaction pathway. In this study we investigate synthesis, crystal structure and magnetic properties of two novel iron(III) complexes and provide some comparison to literature data using correlations previously developed for other class of iron(III) dimers.

2. Experimental

2.1. Materials

1,2-Diamino-2-methylpropane, 5-chlorosalicylaldehyde, 2,2-dimethyl-1,3-propanediamine and $FeCl_3$ have been purchased from

* Corresponding author. Tel.: +90 266 6121000; fax: +90 266 6121215.
E-mail addresses: yaseminyahsi@hotmail.com, yahsi@balikesir.edu.tr (Y. Yahsi).

0020-1693/$ - see front matter © 2010 Elsevier B.V. All rights reserved.
doi:10.1016/j.ica.2010.10.027

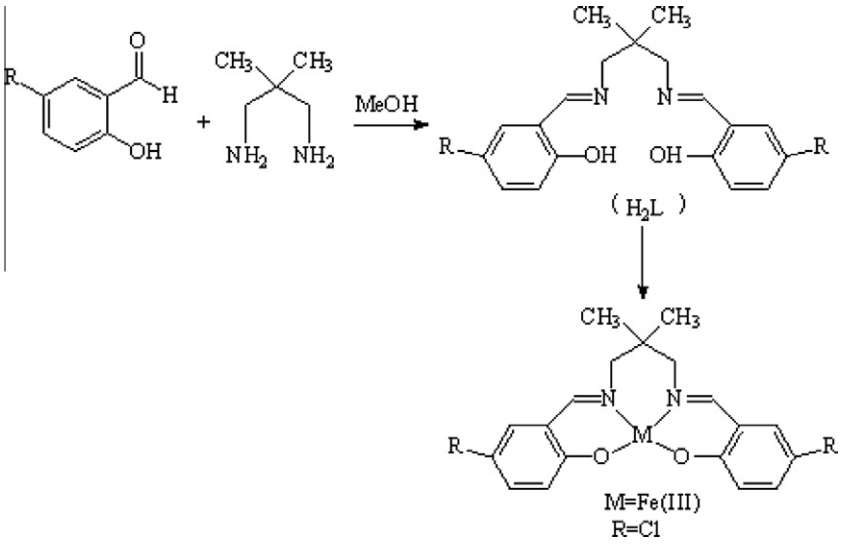

Scheme 1. Schematic diagram of salicylaldimine ligands.

Aldrich Chemical Co. Ethanol has been purchased from Riedel. Elemental (C, H and N) analyses have been carried out by standard methods.

2.2. Synthesis of complex (*1*)

The ligand (H_2L1; *N*,*N*′-bis-(5-chlorosalicylidene)-2-methylpropane-1,2-diamine) has been prepared by reaction of 1,2-diamino-2-methylpropane (1 mmol) with 5-chlorosalicylaldehyde (2 mmol) in hot ethanol (40 mL). The yellow product of H_2L1 was precipitated from solution on cooling. The compound (**1**) has been prepared by addition of $FeCl_3$ (1 mmol) in 20 mL of hot ethanol to H_2L1 (1 mmol) in 40 mL of hot ethanol. This solution has been warmed to 60 °C and stirred for 2 h. The resulting solution has been filtered rapidly and then allowed to stand at room temperature. Several weeks of standing have led to the growth of black crystals of (**1**) suitable for X-ray analysis. *Anal.* Calc. for $C_{18}H_{17}Cl_3N_2O_2Fe$: C, 47.46; H, 3.76; N, 6.15. Found: C, 46.96; H, 3.87; N, 6.21%. UV–Vis (methanol): 234, 310 and 525 nm.

2.3. Synthesis of complex (*2*)

The ligand (H_2L2; *N*,*N*′-bis-(5-chlorosalicylidene)-2,2-dimethylpropane-1,3-diamine) has been prepared by reaction of 2,2-dimethyl-1,3-propanediamine (1 mmol) with 5-Chlorosalicylaldehyde (2 mmol) in hot ethanol (35 mL). The yellow product of H_2L2 was precipitated from solution on cooling. The compound (**2**) has been prepared by addition of $FeCl_3$ (1 mmol) in 20 mL of hot ethanol to H_2L2 (1 mmol) in 30 mL of hot ethanol. This solution has been warmed to 50 °C and stirred for 30 min. The resulting solution has been filtered rapidly and then allowed to stand at room temperature. Two weeks of standing have led to the growth of dark-red crystals of (**2**) suitable for X-ray analysis. *Anal.* Calc. for $C_{38}H_{36}N_4O_4Cl_6Fe_2$; C, 48.70; H, 3.87; N, 5.98. Found: C, 48.35; H, 3.99; N, 5.81%. UV–Vis (methanol): 225, 325 and 564 nm.

2.4. X-ray crystallography

Intensity data for suitable single crystals of the complex (**1**) and complex (**2**) were collected using Stoe-IPDS-2 and Oxford Diffraction Xcalibur-3 diffractometer, respectively, both equipped with a Mo Kα radiation source (λ = 0.71073 Å at 296 K). The data collections and data reductions were performed with the Stoe X-AREA and Stoe X-RED [30] programs for complex **1** and with the CRYSALIS CCD and CRYSALIS RED programs for complex **2** [31], respectively.

The structures were solved by direct methods and refined using full-matrix least-squares against F^2 using SHELXTL [32]. All non-hydrogen atoms were assigned anisotropic displacement parameters and refined without positional constraints. Hydrogen atoms were included in idealised positions with isotropic displacement parameters constrained to 1.5 times the U_{eq} of their attached carbon atoms for methyl hydrogens, and 1.2 times the U_{eq} of their attached carbon atoms for all others. The crystallographic data and some selected bond lengths and angles for both complexes are listed briefly in Tables 1 and 2, respectively. Molecular drawings were obtained using MERCURY [33]. The molecular structures with atom numbering scheme and their packing diagrams are given in Figs. 1 and 2 for complex (**1**) and in Figs. 3 and 4 for complex (**2**), respectively.

2.5. Physical measurements

Magnetization of a sample powder of (**1**) and (**2**) was measured between 2 and 300 K with an applied magnetic field H = 10 kOe using a Cryogenic S600 SQUID magnetometer. The effective magnetic moments were calculated by the equation $\mu_{eff} = 2.828\ (\chi_m T)^{1/2}$ [34], where χ_m, the molar magnetic susceptibility, was set equal to M_m/H. UV–Vis spectra was recorded on Perkin–Elmer Lambda 25 spectrophotometer. IR spectra was recorded on a Perkin–Elmer 1600 series automatic recording FT-IR spectrophotometer with the KBr disk technique in the range of 400–4000 cm^{-1}.

3. Results and discussion

3.1. Crystal structure description of (1)

The result of the X-ray structure solution of complex (**1**) shows (Fig. 1) that the Schiff base ligand coordinates toward one iron atom in a tetradentate mode and each iron atom is five coordinated. In compound (**1**) the equatorial sites are occupied by the N_2O_2 donor atoms of the Schiff base ligand, with average bond distances of Fe–N = 2.081 and Fe–O = 1.894 Å, and the apical chloride atom with Fe–Cl = 2.237 Å.

The crystal packing of square planar complexes of Fe(III) shows a tendency for the formation of stacked structures with

Table 1
Crystal data and structure refinements for (**1**) and (**2**).

	1	2
Empirical formula	$C_{18}H_{16}Cl_3N_2O_2Fe$	$C_{38}H_{36}Cl_6N_4O_4Fe_2$
T (K)	293	293
Formula weight ($g\,mol^{-1}$)	454.53	937.11
Crystal system	monoclinic	triclinic
Space group	$P2_1/c$	$P\bar{1}$
Unit cell dimensions		
a (Å)	8.7404 (7)	8.4434(3)
b (Å)	15.4692 (11)	9.2890(5)
c (Å)	14.5641 (12)	12.6005(6)
α (°)		82.085(5)
β (°)	107.045 (6)	79.107(4)
γ (°)		86.436(4)
V (Å^3)	1882.7 (3)	960.55(8)
Z	4	1
D_{calc} ($g\,cm^{-3}$)	1.604	1.620
Absorption coefficient (mm^{-1})	1.24	1.22
θ range for data collection	2–27.1°	3.7–32.3°
Index ranges	$-11 \leqslant h \leqslant 11$ $-19 \leqslant k \leqslant 19$ $-18 \leqslant l \leqslant 18$	$-12 \leqslant h \leqslant 12$ $-13 \leqslant k \leqslant 13$ $-18 \leqslant l \leqslant 18$
Reflections collected	21404	11970
Independent reflections	4066 [R_{int} = 0.153]	6166 [R_{int} = 0.0219]
Refinement method	Full-matrix least-squares on F^2	Full-matrix least-squares on F^2
Goodness-of-fit on (GOF) F^2	S = 1.08	S = 0.929
R indices [$I > 2\sigma(I)$]	R_1 = 0.117, wR_2 = 0.321	R_1 = 0.032, wR_2 = 0.078

metal···metal or metal···ligand intermolecular short cut distances. Moreover, infinite chains or dimers may be formed. For (**1**), although the coordination geometry around iron atom can be described as a distorted square pyramid, non-bonding interaction results in this mononuclear Fe(III) complex adopting a dimeric structure, with non-bonding interatomic Fe···O and Fe···Fe separations of 2.894 and 3.773 Å, respectively. As shown in molecular packing diagram of (**1**) (Fig. 2), dimeric units are linked by inversion centers and neighboring dimers are linked by infinite zig-zag chains through weak ligand–ligand interactions with the distance of Cl2···$Cl3_{1+x,1+y,z}$ equal to 3.495 Å. The Fe···Fe separation of complex (**1**) with 3.773 Å is similar to that observed in some carboxylato-bridged dinuclear Fe(III) complexes [25,26,35,36] and it is longer than the value of compound (**2**) (3.341 Å).

3.2. Crystal structure description of (2)

The molecular structure of compound (**2**) obtained by X-Ray diffractometry (Fig. 3) shows that the complex is a centrosymmetric dimer in which the six coordinated Fe(III) atoms are linked by μ-phenoxo bridges from one of the phenolic oxygen atoms of each Schiff base ligand to the opposite metal center, thus resulting in μ-phenoxo Fe1–O1A and Fe1A–O1 bond distances of 2.244 (11) Å. The environment around each iron atom can be described as a distorted octahedral geometry. The octahedral coordination of each Fe(III) ion is completed by a tetradentate Schiff base ligand and a terminal Cl^- ion. The two Cl^- ligands are exactly *trans* about the Fe···Fe vector, due to the inversion centre.

In the Fe_2O_2 bridging moiety, which is strictly planar due to the centrosymmetry, the Fe1–O_{bridge}–Fe1A angle is 103.83 (4)° and the Fe1···Fe1A distance is 3.341 Å. The Fe···Fe separation is slightly longer than the corresponding ones of similar dinuclear iron(III) complexes (3.291, 3.339, 3.189 and 3.165 Å) [25,26,35,36]. The plane defining the Fe1–O1–Fe1A–O1A bridge makes an angle of 85.36° and 89.28° with the equatorial coordination plane defined by the atoms Fe1, N1, N2, O1 and Fe1, N1, N2, O2, respectively. However, the angle between these equatorial planes is 3.95°. In the equatorial plane Fe–O(phenoxo) [Fe–O1 = 1.996 (10) Å, Fe–O2= 1.890 (10) Å] and Fe–N (imine) [Fe–N1 = 2.136 (12) Å, Fe–N2 = 2.133 (13) Å] bond distances are slightly shorter than the axial Fe–O (μ-phenoxo) [Fe–O1A = 2.244 (11) Å] and Fe–Cl [2.294(5) Å]. And the shortest interdimer Fe···Fe distance is 7.015 Å.

The stacking interaction is also observed in molecular packing of complex (**2**) (Fig. 4). The compound interact with the distances Cl2···$Cl22_{-x,-y,-1-z}$, Cl1···$H10C1_{-x,-y,-z}$, O2···$H18_{-x,1-y,-z}$ and Cl3···$H11A_{-x,1-y,1-z}$ equal to 3.397, 2.868, 2.621 and 2.931 Å, respectively. The neighboring dimers are formed in three-dimensional networks and the closest centroid-to-centroid distance of Fe1–O1–Fe1A–O1A is 9.289 Å. This supramolecular polymeric networks lie in the *ab*-plane and stacks orthogonally to the *c*-axis (Fig. 4). Furthermore, in complex (**2**), there is also face to face π–π stacking interaction between the pyridine rings of the Schiff base ligands. The centroid-to-centroid and centroid-to-plane distances between the intramolecular aromatic rings are 3.550 and 3.344 Å, respectively.

3.3. IR spectra

Infrared spectra of complex (**1**) and (**2**) are shown in Table 3. In the infrared spectrum of the complex (**1**) in KBr disc, a strong band observed at 1619 cm^{-1} is attributed to the C=N stretch which can

Table 2
Some selected bond lengths (Å) and angles (°) for (**1**) and (**2**).

Bond lengths (Å)	(1)	(2)	Bond angles (°)	(1)	(2)
Fe1–O1	1.931 (8)	1.996 (10)	O2–Fe1–O1	98.9 (3)	103.43 (4)
Fe1–O2	1.857 (7)	1.890 (10)	O2–Fe1–N2	89.5 (3)	87.63 (5)
Fe1–N1	2.077 (8)	2.136 (12)	N2–Fe1–N1	76.9 (3)	83.17 (5)
Fe1–N2	2.086 (8)	2.133 (13)	O1–Fe1–N1	85.5 (3)	84.07 (4)
Fe1–Cl1	2.239 (4)	2.294 (5)	O2–Fe1–N1	156.8 (3)	164.84 (5)
Fe1–O1A		2.244 (11)	O1–Fe1–N2	151.4 (4)	165.76 (5)
			O1–Fe1–Cl1	101.4 (3)	95.02 (3)
			O2–Fe1–Cl1	101.7 (3)	96.20 (4)
			N1–Fe1–Cl1	99.7 (3)	96.22 (4)
			N2–Fe1–Cl1	103.6 (3)	92.61 (4)
			O1–Fe1–O1A		76.17 (4)
			O2–Fe1–O1A		86.35 (4)
			Fe1–O1–Fe1A		103.83 (4)
			N1–Fe1–O1A		82.66 (4)
			N2–Fe1–O1A		95.93 (4)

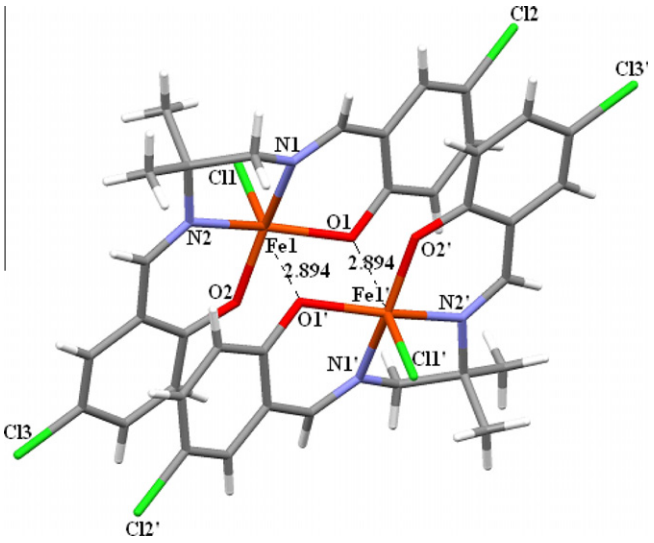

Fig. 1. Molecular structure of (**1**).

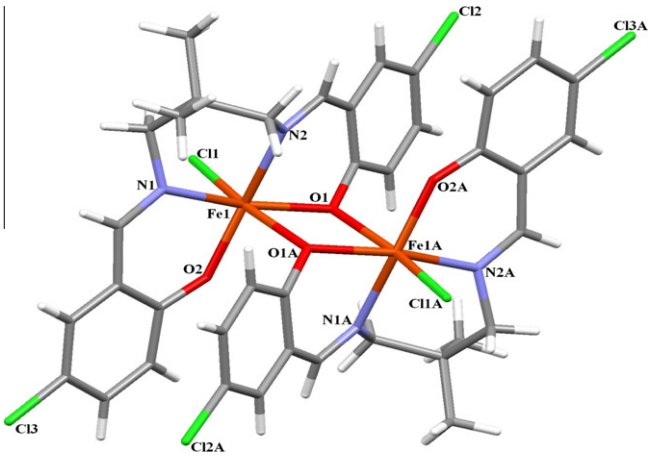

Fig. 3. Molecular structure of (**2**).

be related to the band observed at 1614 cm^{-1} in the spectrum of (**2**). The bands in the range of 2860–2977 cm^{-1} are characteristic of aliphatic ν(C–H) vibrations for complex (**1**) and (**2**) and the band observed at 3080 cm^{-1} is attributed to the aromatic ν(C–H) vibrations for both. The observed bands in the range of 655–716 cm^{-1} are characteristic of ν(C–Cl) vibrations of chlorosalicylideneimine ligands for both complexes.

3.4. Magnetic properties

The variable temperature magnetic susceptibilities for (**1**) and (**2**) were measured in the 4–300 K temperature range and are shown as χ and μ_{eff} versus T plots in Figs. 5 and 6, respectively.

The experimental χ value increases in the range of 4–10 K for (**1**) and of 4–50 K for (**2**) then decreases monotonically up to 300 K for both. The experimental μ_{eff} values for compound (**1**) and (**2**) at room temperature are approximately 7.98 and 7.43 μ_B, respectively, and for lower temperature the magnetic moments smoothly decrease to attain a value of 1.50 μ_B for (**1**) and 1.04 μ_B for (**2**) at 4 K. At room temperature, the observed magnetic moments per dinuclear complexes are slightly lower than the spin only value (8.37 μ_B) expected for a system containing two uncoupled high-spin ($S = 5/2$) iron(III) centers. This result shows that both Fe(III) ions of dinuclear complexes are in the $S = 5/2$ ground state and indicates the presence of an antiferromagnetic spin-exchange interaction between Fe(III) ions in the dimer via bridging oxygen atoms of tetradentate Schiff base ligand.

For diiron(III) complexes ($S1 = S_2 = 5/2$) containing a paramagnetic impurity (ρ), the theoretical expression of the magnetic susceptibility based on the Heisenberg hamiltonian ($\boldsymbol{H} = -2J\boldsymbol{S}_1\boldsymbol{S}_2$) is:

$$\chi = \frac{Ng^2\mu_B^2}{kT} \times \frac{[2e^{2x} + 10e^{6x} + 28e^{12x} + 60e^{20x} + 110e^{30x}]}{[1 + 3e^{2x} + 5e^{6x} + 7e^{12x} + 9e^{20x} + 11e^{30x}]} \times (1 - \rho) + \frac{Ng^2\mu_B^2}{3k(T - \theta)} S(S + 1) \times \rho$$

where $x = J/kT$. In this expression all symbols have their usual meaning, θ is a Weiss-like correction to account for possible intermolecular exchange effects. These corrections are usually small

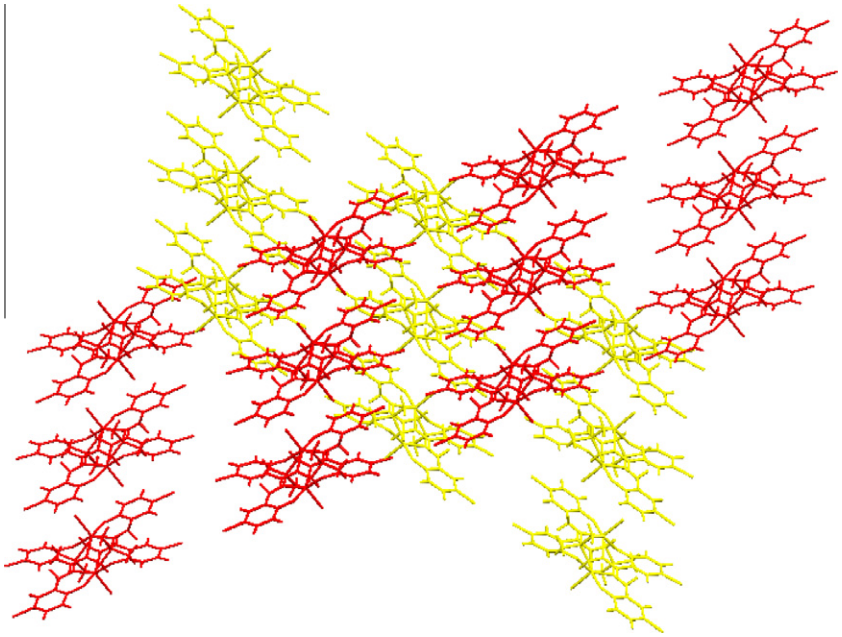

Fig. 2. Molecular packing diagram of (**1**).

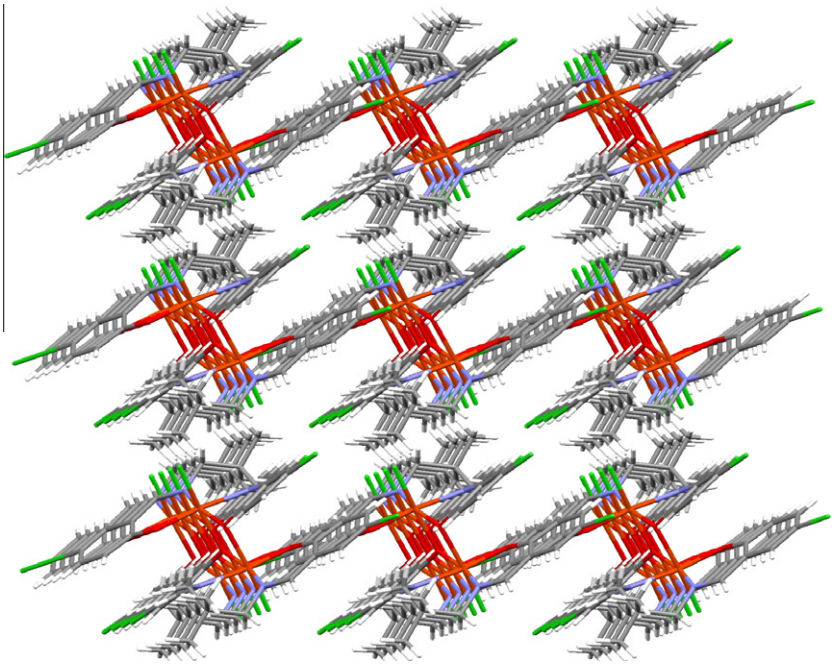

Fig. 4. Molecular packing diagram of (**2**).

Table 3
Infrared spectra of complex (**1**) and (**2**).

Complex	ν(C–H) (cm^{-1}) (aromatic)	ν(C–H) (cm^{-1}) (aliphatic)	ν(C=N) (cm^{-1})	ν(C–Cl) (cm^{-1})
(**1**)	3080	2977, 2911	1619	710, 690, 659
(**2**)	3080	2955, 2910, 2860	1614	716, 655

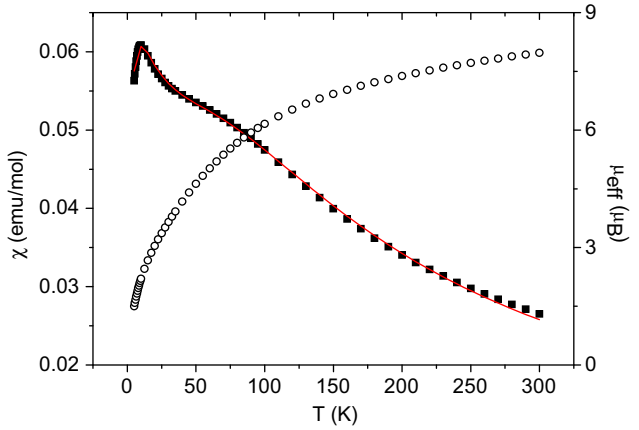

Fig. 5. Temperature variation of the magnetic susceptibilities and magnetic moments of (**1**) as χ (■) and μ_{eff} (o) vs. T plots. The solid line represents the best fit of the experimental data based on the Heisenberg model (for χ).

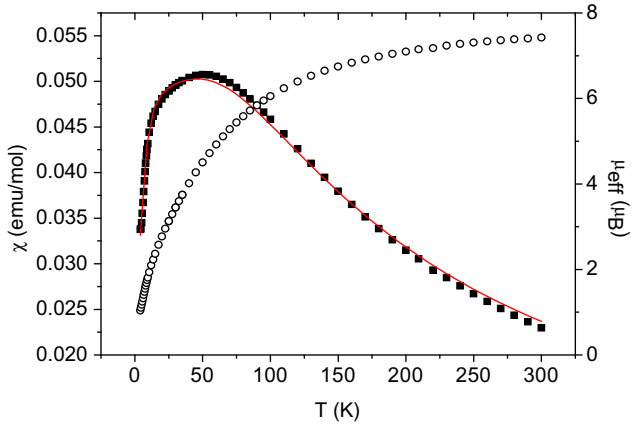

Fig. 6. Temperature variation of the magnetic susceptibilities and magnetic moments of (**2**) as χ (■) and μ_{eff} (o) vs. T plots. The solid lines represent the best fit of the experimental data based on the Heisenberg model (for χ).

and may result from weak lattice associations or hydrogen-bonding interactions [37]. The best agreement with the experimental data was obtained for $J = -7.49 \pm 0.07$ cm^{-1}, $g = 2.14 \pm 0.007$, $\rho = 0.089 \pm 0.003$, $\theta = -4.1 \pm 0.3$ K for complex (**1**) and $J = -6.44 \pm 0.04$ cm^{-1}, $g = 1.984 \pm 0.004$, $\rho = 0.018 \pm 0.001$, $\theta = 1.05 \pm 0.1$ K for complex (**2**) ($R^2 = 0.99849$). As a whole, these results indicate a significant antiferromagnetic coupling in dinuclear units. The relatively high percentage of paramagnetic impurity for complex (**1**), resulting from the presence of mononuclear Fe(III) molecules, may probably be the reason of the unphysical g value obtained by the fitting procedure. We note here that performing the fitting by constraining g value to be fixed at 2.0 results in a lower quality fit for **1** with $J = -6.5 \pm 0.07$ cm^{-1}, $\rho = 0.074 \pm 0.003$, $\theta = -2.5 \pm 0.3$ K, while the fit for **2**, essentially of the same quality of the one obtained with free g value, provides $J = -6.5 \pm 0.07$ cm^{-1}, $\rho = 0.01 \pm 0.003$, $\theta = 0.7 \pm 0.1$ K. Given the relatively high θ/J ratio for (**1**), and the uncertainty on the actual parameters, we will not consider the obtained results in the analysis of possible magnetostructural correlations in the following. On the other hand the small Weiss-like corrections for complex (**2**) indicate the presence of non-negligible intermolecular interactions, which are reasonably associated with the stacking interactions between two neighboring complexes.

The interpretation of magnetostructural correlations in dinuclear and polynuclear iron(III) complexes still lacks a firm and simple theoretical interpretation. The main reason for this is the large number of magnetic orbitals, and thus of interactions, which concurs to the global coupling. Thus magnetostructural correlations

for exchange-couplediron(III) centres are usually restricted to an empirical or semi-empirical approach. In particular, different structural features were found to affect the strength of antiferromagnetic super-exchange coupling constant. Among these, the most relevant are the planarity of the bonds around the bridging oxygen atom, the Fe···Fe distance, the ⟨Fe–O⟩ average bond lengths between the iron and the bridging oxygen atoms and the Fe–O–Fe bridging angle: however, their relative contribution to the resulting coupling is still debated [38,39]. As an example, an extensive group of hydroxide-, alkoxide- and phenoxide-bridged iron(III) dimers was studied by Haase and co-workers, [39] who concluded that angular dependence is small. This was contrasted by the results reported by other authors, especially Le Gall et al. [38]. More recently Alvarez adopted as relevant structural parameter which determine the coupling strength the ratio between the average Fe–O–Fe bond angle and the Fe–O bond distance, and obtained a fair correlation with the *J* value [40].

The selected structural and magnetic data of (**2**) and related complexes reported in literature are listed in Table 4 and the correlation diagrams of *J* versus Fe···Fe distance and ⟨Fe–O⟩ bond length are presented in Figs. 7 and 8, respectively. The solid line drawn as a guide shows a correlation between the antiferromagnetic super-exchange coupling constant *J* and the structural data of dimeric Fe(III) complexes. This guide allows us to notice that an increase of the Fe···Fe distance and ⟨Fe–O⟩ average bond distance corresponds a decrease of the antiferromagnetic exchange integral. However there is no simple correlation of the Fe–O–Fe bridging angle with the strength of the exchange interaction. Thus, the large average bond lengths between the iron and the bridging oxygen atoms and also the large intramolecular Fe···Fe distance are responsible for the relatively weak antiferromagnetic coupling. In complex (**2**) and the similar compounds, in spite of the influence of the ⟨Fe–O⟩ and Fe···Fe distance on the strength of the antiferromagnetic super-exchange coupling, there is no certain relation between structural parameters and the value of the coupling constant.

Table 4
Structural and magnetic data of the related compounds.

Compound	Fe···Fe (Å)	Fe–O–Fe (°)	<Fe–O> (Å)	J (cm^{-1})
a[41]	3.118	105.3	1.962	−11.7
b[42]	3.089	103.6	1.966	−11.4
c[43]	3.116	103.6	1.982	−11.0
d[23]	3.196	105.8	2.003	−10.1
e[35]	3.189	104.3	2.020	−8.3
f[25]	3.291	105	2.080	−7.5
g[26]	3.339	104.08	2.115	−6.85
(**2**)	3.341	103.83	2.120	−6.37

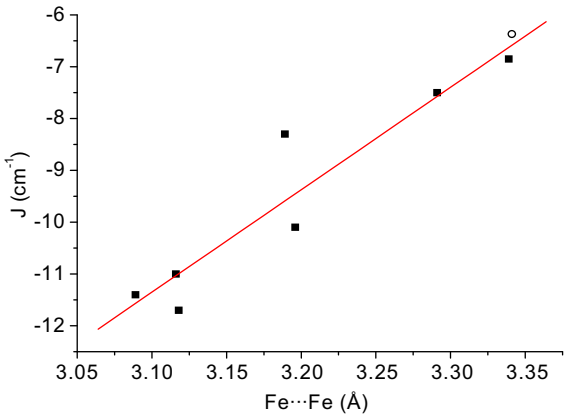

Fig. 7. A plot of Fe···Fe distance vs. the exchange interactions (*J*); squares are literature data listed in Table 3 and circle is for complex (**2**); the solid line is drawn only as a guide.

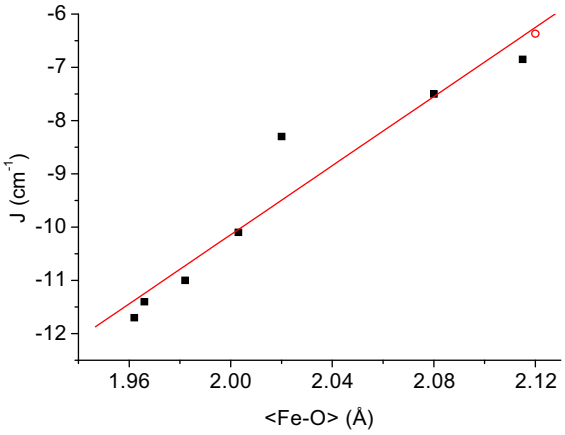

Fig. 8. A plot of ⟨Fe–O⟩ average bond distance vs. the exchange interactions (*J*); squares are literature data listed in Table 3 and circle is for complex (**2**); the solid line is drawn only as a guide.

4. Conclusions

Two new complexes have been obtained with the tetradentate Schiff Base ligand. The first one is a mononuclear complex (**1**) which has been characterized by elemental analysis, single crystal X-ray, FT-IR and UV–Vis. As shown in the packing diagram of (**1**), this momomeric Fe(III) complex with very close non-bonding interatomic Fe···O distance resembles dimeric iron complex. The second one is a phenoxo-bridged diiron(III) complex (**2**) and has also been characterized by the same techniques with (**1**). The infrared and electronic spectra of both Fe(III) complexes are also similar. The exchange coupling constants (*J*) have been found to be $-7.49\ cm^{-1}$ for (**1**) and $-6.44\ cm^{-1}$ for (**2**), evidencing that the metal centers of these two complexes are weakly antiferromagnetically coupled. It is however to be noted that the uncertainty on the parameters obtained for the weakly associated dimer (**1**) is quite relevant, due to the presence of a large fraction of paramagnetic impurity. On the other hand when compared to literature data, the results obtained for (**2**) indicates that both the bond lengths between the iron and the bridging oxygen atoms and the Fe···Fe distance are the longest hitherto reported, and should then be considered responsible for the relatively weak antiferromagnetic coupling observed.

Acknowledgements

The authors are grateful to the Research Funds of Balikesir University (BAP-2007/06) for the financial support and to the Faculty of Arts and Sciences, Ondokuz Mayis University, for the use of STOE IPDS II diffractometer (purchased under grant F.279 of the University Research Fund). Yasemin Yahsi is also grateful to the European Union Erasmus Program for the financial support and to Laboratory of Molecular Magnetism (Department of Chemistry, University of Florence) for the use of Xcalibur-3 diffractometer and Cryogenic S600 SQUID magnetometer.

Appendix A. Supplementary material

CCDC 780445 (**1**) and 780446 (**2**) contains the supplementary crystallographic data for this paper. These data can be obtained free of charge from The Cambridge Crystallographic Data Centre via www.ccdc.cam.ac.uk/data_request/cif. Supplementary data

associated with this article can be found, in the online version, at doi:10.1016/j.ica.2010.10.027.

References

[1] R.H. Holm, G.W. Everett Jr., A. Chakavorty, Prog. Inorg. Chem. 7 (1966) 83.
[2] E.N. Jacobsen, in: E.W. Abel, F.G.A. Stone, G. Wilkinson (Eds.), Comprehensive Organometallic Chemistry, vol. 12, Elsevier, New York, 1995.
[3] M.A. Torzilli, S. Colquhoun, J. Kim, R.H. Beer, Polyhedron 21 (2002) 705.
[4] H. Fujii, T. Kurahashi, T. Ogura, J. Inorg. Biochem. 96 (2003) 133.
[5] L. Que Jr., Coord. Chem. Rev. 50 (1983) 73.
[6] H. Fujii, Y. Funahashi, Angew. Chem., Int. Ed. 41 (2002) 3638.
[7] K.P. Bryliakov, E.P. Talsi, Angew. Chem., Int. Ed. 43 (2004) 5228.
[8] T. Katsuki, Chem. Soc. Rev. 33 (2004) 437.
[9] A. Boettcher, M.W. Grinstaff, J.A. Labinger, H.B. Gray, J. Mol. Catal. A Chem. 113 (1996) 191.
[10] B.J. Kennedy, A.C. McGrath, K.S. Murray, B.W. Skelton, A.H. White, Inorg. Chem. 26 (1987) 483.
[11] P.J. Nichols, G.D. Fallon, K.S. Murray, B.O. West, Inorg. Chem. 27 (1988) 2795.
[12] C.T. Brewer, G. Brewer, G.B. Jameson, P. Kamaras, L. May, M. Rapta, J. Chem. Soc., Dalton Trans. (1995) 37.
[13] W. Chiang, D. Vanengen, M.E. Thompson, Polyhedron 15 (1996) 2369.
[14] M.M. Bhadbhade, D. Srinivas, Polyhedron 17 (1998) 2699.
[15] S. Hayami, K. Inoue, Y. Maeda, Mol. Cryst. Liq. Cryst. 335 (1999) 1285.
[16] S.J. Lippard, Angew. Chem. Int. Ed. Engl. 27 (1988) 344.
[17] S.M. Gorun, S.J. Lippard, Inorg. Chem. 30 (1991) 1625.
[18] L. Borer, L. Thalken, C. Cecarelli, M. Glick, J.H. Zhang, W.M. Reiff, Inorg. Chem. 22 (1983) 1719.
[19] H. Weihe, H.U. Gudel, J. Am. Chem. Soc. 119 (1997) 6539.
[20] H.J. Schugar, G.R. Rossman, H.B. Gray, J. Am. Chem. Soc. 91 (1969) 4564.
[21] A.S. Attia, M.F. El-Shahat, Polyhedron 26 (2007) 791.
[22] Z.L. You, H.L. Zhu, Acta Crystallogr., Sect. E60 (2004) m1046.
[23] A. Elmali, Y. Elerman, C.T. Zeyrek, I. Svoboda, Z. Naturforsch. 58b (2003) 433.
[24] W.M. Reiff, G.J. Long, W.A. Baker, J. Am. Chem. Soc. 90 (1968) 6347.
[25] M. Gerloch, F.E. Mabbs, J. Chem. Soc. (A) 1 (1967) 1900.
[26] Y. Yahsi, H. Kara, C. Kazak, A. Iakovenko, L. Sorace, J. Optoelectr. Adv. Mater. Symp. 1 (2009) 566.
[27] A. Geiß, H. Vahrenkamp, Eur. J. Inorg. Chem. (1999) 1793.
[28] J.L. Resce, J.C. Fanning, C.S. Day, S.-J. Uhm, A.F. Croisy, L.K. Keefer, Acta Crystallogr., Sect. C43 (1987) 2100.
[29] M. Mikuriya, Y. Kakuta, R. Nukada, T. Kotera, T. Tokii, Bull. Chem. Soc. Jpn. 74 (2001) 1425.
[30] Stoe&Cie X-AREA (Version 1.18) and X-RED (Version 1.04), Stoe & Cie, Darmstadt, Germany, 2002.
[31] Oxford Diffraction Ltd., Version 1.171.31.2.
[32] SHELXTL, Rev. 5.0, Bruker AXS, Madison, WI, USA.
[33] MERCURY 1.4.2, Copyright from CCDC 2001–2007.
[34] O. Kahn, Molecular Magnetism, VCH publishers, New York, 1993.
[35] A. Elmali, Y. Elerman, I. Svoboda, H. Fuess, J. Mol. Struct. 516 (2000) 43.
[36] E.Q. Gao, L.H. Yin, J.K. Tang, P. Cheng, D.Z. Liao, Z.H. Jiang, S.P. Yan, Polyhedron 20 (2001) 669.
[37] K. Costuas, M.L. Valenzuela, A. Vega, Y. Moreno, O. Pena, E. Spodine, J.Y. Saillard, C. Diaz, Inorg. Chim. Acta 329 (2002) 129.
[38] F. Le Gall, F.F. de Biani, A. Caneschi, P. Cinelli, A. Cornia, A.C. Fabretti, D. Gatteschi, Inorg. Chim. Acta 262 (1997) 123.
[39] R. Werner, S. Ostrowvsky, K. Griesar, W. Haase, Inorg. Chim. Acta 326 (2001) 78.
[40] E. Ruiz, S. Alvarez, ChemPhysChem 6 (2005) 1094.
[41] C.C. Ou, R.A. Lalancette, J.A. Potenza, H.J. Schugar, J. Am. Chem. Soc. 100 (1978) 2053.
[42] J.A. Thich, C.C. Ou, D. Powers, B. Vasiliou, D. Mastropaolo, J.A. Potenza, H.J. Schugar, J. Am. Chem. Soc. 98 (1976) 1425.
[43] B. Chiari, O. Piovesana, T. Tarantelli, P.F. Zanazzi, Inorg. Chem. 23 (1984) 3398.